J. Fluid Mech. (1977), *vol.* 80, *part* 4, *pp.* 673–683
Printed in Great Britain

The round laminar jet: the development of the flow field

By C. SOZOU AND W. M. PICKERING

Department of Applied Mathematics and Computing Science,
University of Sheffield, England

(Received 26 November 1976)

The development of the flow field of a jet emanating from a point source of momentum in an infinite incompressible fluid of density ρ is considered. The flow field is assumed to be due to the application of a constant force F_0 at the origin. The problem is formulated in terms of the dimensionless variable $\lambda = (\nu t)^{\frac{1}{2}}/r$, where ν is the kinematic viscosity of the fluid, t the time from the application of the force and r the distance from the origin. At a station r the flow field is dipolar, with the dipole axis in the direction of F_0, for all t satisfying the inequalities $\nu t \ll r^2$ and $F_0 t^2 \ll 4\pi\rho r^4$. Also, at a given time t the streamlines of the developing flow field in a section through the axis of symmetry of the problem form closed loops about a stagnation point. If this occurs at $\lambda = \lambda_m$, the stagnation point propagates to infinity, along a straight line emanating from the origin, with speed $\nu^{\frac{1}{2}}/2\lambda_m t^{\frac{1}{2}}$, where $\lambda_m = \lambda_m(F_0)$ decreases as F_0 increases. The larger F_0 is the faster the steady state is established.

1. Introduction

The steady-state flow field of a point source of momentum was considered by Landau in 1944 (see Landau & Lifshitz 1959, p. 86) and by Squire (1951) and represents one of the few exact solutions of nonlinear axisymmetric hydrodynamics. The jet is generated by the action of a force F_0 applied at one point. This jet was reviewed by Batchelor (1967, p. 205), who showed that its flow pattern is the same as that generated by a slow-moving body at large distances from the body, where the actual body shape is irrelevant, provided that $2\pi\rho\nu^2 \ll F_0$ = drag experienced by the body. Also it was recently suggested by Lighthill (1973) that the far flow field generated by a small hovering insect of weight w, such as *Encarsia formosa*, will take the form of this classical round laminar jet provided that $w/\rho\nu^2$ is sufficiently small that the flow field generated is stable.

The development of the flow field of the momentum jet has never been considered. This we investigate in the present paper. We show that initially the force sets up an impulsive pressure, generating a dipole-like field. However, the equations describing the development are in general of mixed type and rather complicated, and even in the linear case must be solved numerically. We recently considered a very similar set of equations, concerning the development of the flow field due to an electric current discharge in a semi-infinite medium (Sozou & Pickering 1975). Thus, here we follow the same general approach, making use of the same numerical techniques, and solve our equations by iteration.

2. Formulation of the problem

We consider an incompressible fluid of infinite extent which is acted on by a force $\mathbf{F}_0$ at the origin of a spherical polar co-ordinate system (r, θ, ϕ), the direction of the force being along the axis $\theta = 0$. We assume that F_0 is suddenly switched on and wish to investigate the development of the flow field being set up. The velocity field will obviously be symmetric about the axis $\theta = 0, \pi$ and, on dimensional grounds, the stream function ψ associated with this will be given by

$$\psi = \nu r g(\mu, \lambda), \tag{1}$$

where ν is the kinematic viscosity of the fluid, $\mu = \cos\theta$ and $\lambda = (\nu t)^{\frac{1}{2}}/r$. Thus the fluid velocity $\mathbf{v}$ will be given by

$$\mathbf{v} = -\nu r^{-1}[g_\mu, (g - \lambda g_\lambda)/(1-\mu^2)^{\frac{1}{2}}, 0], \tag{2}$$

where a suffix denotes partial differentiation with respect to that variable. The momentum equation is

$$\partial \mathbf{v}/\partial t + (\nabla \times \mathbf{v}) \times \mathbf{v} = -\nabla(p/\rho + \tfrac{1}{2}v^2) + \nu \nabla^2 \mathbf{v}, \tag{3}$$

where p and ρ are the fluid pressure and density respectively. On dimensional grounds, apart from an additive constant,

$$p = \nu^2 \rho h(\mu, \lambda)/r^2. \tag{4}$$

On taking the curl of (3) and making use of (2), after some manipulation we obtain

$$(1-\mu^2) f_{\mu\mu} - 4\mu f_\mu + \lambda^2 f_{\lambda\lambda} + (4\lambda - 1/2\lambda) f_\lambda - 3f g_\mu - g f_\mu - \lambda(f_\lambda g_\mu - f_\mu g_\lambda) = 0, \tag{5}$$

where

$$g_{\mu\mu} + \lambda^2 g_{\lambda\lambda}/(1-\mu^2) = f(\mu, \lambda). \tag{6}$$

Equations (5) and (6) are the governing equations of our problem. These equations are very similar to a pair of equations used in our previous investigation of the development of the magnetohydrodynamic flow field due to an electric current discharge in a conducting semi-infinite fluid. On correcting a misprint in our previous equation (6) and setting a constant K, which is related to the contribution of the electromagnetic field, equal to zero that equation reduces to our present equation (5). Our present equation (6) is identical to our previous equation (7). Thus, as before, we assume that for a fixed r as $t \to \infty$, i.e. as $\lambda \to \infty$, the λ dependence of the solution will die out exponentially. This implies, of course, that as $\lambda \to \infty$

$$\lambda f_\lambda, \lambda^2 f_{\lambda\lambda}, \lambda g_\lambda, \lambda^2 g_{\lambda\lambda} \to 0. \tag{7}$$

On eliminating f between (5) and (6), making use of (7), we find that the steady-state solution $g_\infty(\mu, \infty)$ satisfies the equation

$$(1-\mu^2) g_\infty^{\mathrm{iv}} - 4\mu g_\infty''' - 3 g_\infty' g_\infty'' - g_\infty g_\infty''' = 0, \tag{8}$$

where a prime denotes differentiation. The appropriate solution of (8) such that the velocity field has no singularities on $\mu = \pm 1$ (Whitham 1963; Batchelor 1967, p. 207) is

$$g_\infty = 2(1-\mu^2)/(1+c-\mu), \tag{9}$$

where c is a constant related to the force F_0 inducing the flow by the equation

$$\frac{F_0}{2\pi\rho\nu^2} = \frac{32}{3}\frac{1+c}{c(2+c)} + 4(1+c)^2 \log\left(\frac{c}{2+c}\right) + 8(1+c). \tag{10}$$

Equations (5) and (6) must, of course, be solved numerically in the region $-1 \leqslant \mu \leqslant 1, 0 \leqslant \lambda \leqslant \infty$. It is not easy to solve (5) and (6) in the semi-infinite interval $0 \leqslant \lambda \leqslant \infty$. The assumption that the dependence of f and g on λ dies out exponentially as $\lambda \to \infty$ enables us to solve (5) and (6) in the strip $-1 \leqslant \mu \leqslant 1, 0 \leqslant \lambda \leqslant \Lambda$, where Λ is a finite quantity. This assumption is justified *a posteriori* by our results.

If we assume that g is specified, (5) is a linear equation in f which is elliptic in the region of interest and parabolic on $\lambda = 0$ and on $\mu = \pm 1$. Similarly, if we assume that f is specified, (6) is a linear elliptic equation in g which becomes parabolic on $\lambda = 0$ and on $\mu = \pm 1$. We can therefore solve our problem iteratively as follows: we specify g and solve (5) for f. That solution is used in (6) to construct a better approximation to g, which is then used in (5) for a better approximation to f and so on.

The boundary conditions on f and g for the solution of (5) and (6) are

$$f(\mu, 0) = 0, \quad g(\mu, 0) = 0, \quad g(1, \lambda) = g(-1, \lambda) = 0, \tag{11)-(13}$$

$$g(\mu, \Lambda) = g_\infty(\mu), \quad f(\mu, \Lambda) = g''_\infty(\mu), \tag{14), (15}$$

$$\mp 4f_\mu + \lambda^2 f_{\lambda\lambda} + (4\lambda - 1/2\lambda) f_\lambda - 3fg_\mu - \lambda f_\lambda g_\mu = 0 \quad \text{on} \quad \mu = \pm 1. \tag{16), (17}$$

Equations (11) and (12) mean that f and g are zero at $t = 0$ and (13) implies that $\mathbf{v}$ [see (2)] is finite on the axis of symmetry of the problem $\mu = \pm 1$. Equations (14) and (15) imply approximation of $g(\mu, \infty)$ by $g(\mu, \Lambda)$ and of $f(\mu, \infty)$ by $f(\mu, \Lambda)$. Equations (16) and (17) are derived from (5) and (13) on the assumption that $f_{\mu\mu}$ is finite on $\mu = \pm 1$. This is a reasonable assumption, since when $\lambda = \infty$, $f_{\mu\mu}$ is finite on $\mu = \pm 1$ and we cannot see any reason why $f_{\mu\mu}$ should not be finite on $\mu = \pm 1$ for all λ.

On considering the radial component of (3), we obtain

$$\left(1 + \frac{\lambda}{2}\frac{\partial}{\partial\lambda}\right)\left[2h + g_\mu^2 + \frac{(g - \lambda g_\lambda)^2}{1 - \mu^2}\right] = -\frac{1}{2\lambda} g_{\lambda\mu} - f(g - \lambda g_\lambda) + \frac{\partial}{\partial\mu}[(1 - \mu^2) f].$$

Hence, by integration,

$$h = h^* - \tfrac{1}{2} g_\mu / \lambda^2, \tag{18}$$

where

$$h^* = -\frac{1}{2}\left[g_\mu^2 + \frac{(g - \lambda g_\lambda)^2}{1 - \mu^2}\right] - \frac{1}{\lambda^2}\int_0^\lambda \lambda [f(2\mu + g - \lambda g_\lambda) - (1 - \mu^2) f_\mu]\, d\lambda. \tag{19}$$

From (6), (7) and (19) it can be shown that, in the limit when $\lambda \to \infty$, h tends to its steady-state value h_∞, for which an expression is given in Batchelor's book (p. 207):

$$h(\mu, \infty) = h_\infty = -\frac{1}{2}\frac{g_\infty^2}{1 - \mu^2} - \frac{1}{2}\frac{d}{d\mu}[g_\infty g'_\infty - (1 - \mu^2) g''_\infty] = \frac{4[(1 + c)\mu - 1]}{(1 + c - \mu)^2}. \tag{20}$$

The approximate satisfaction of

$$h(\mu, \Lambda) = h_\infty \tag{21}$$

can be used as an indication of the accuracy of our numerical solution.

On using the fact that the rate of increase of the linear momentum of the fluid in a volume bounded by a surface S is equal to the total force acting on that fluid we can relate the impressed force F_0 to an integral involving the solution we construct. Taking

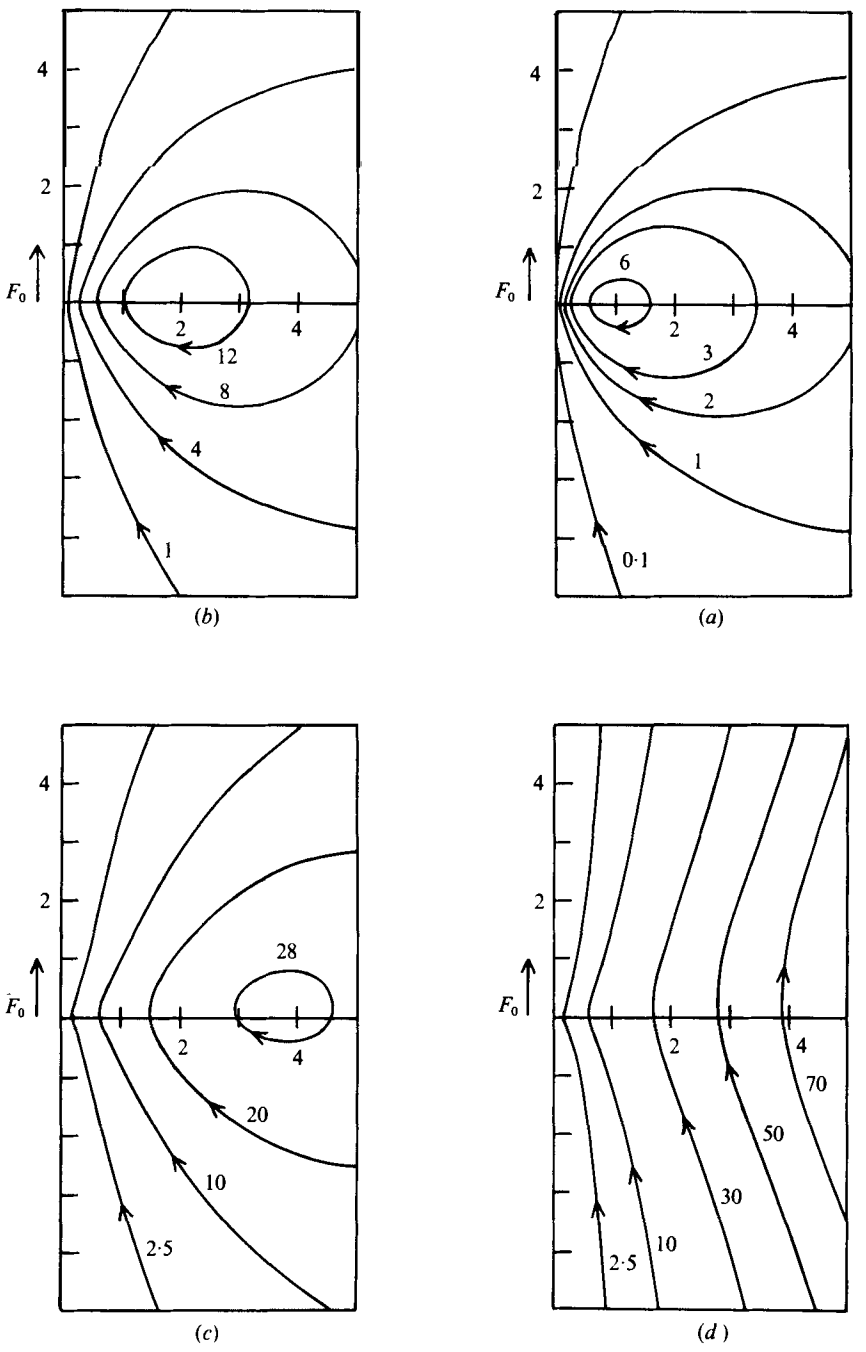

FIGURE 1. Streamlines of the developing flow field for the case $c = 10$ at (*a*) $T = 0{\cdot}5$, (*b*) $T = 1$, (*c*) $T = 2$ and (*d*) $T = \infty$, where $T = (\nu t)^{\frac{1}{2}}/L$ and L is a characteristic length. The numbers on the curves are values of $100\psi/\nu L$. The distances along the axes are in units of L. $F_0 = 1{\cdot}46\pi\rho\nu^2$.

for S the surface of a sphere of radius R surrounding the origin and considering the rate of change of linear momentum in the direction of $\mathbf{F}_0$, we obtain

$$F_0 = \int_\tau \frac{\partial}{\partial t}[\rho(\mathbf{v}.\hat{\mathbf{r}}\cos\theta - \mathbf{v}.\hat{\boldsymbol{\theta}}\sin\theta)]\,d\tau + 2\pi R^2 \int_{-1}^{1} [\rho\mathbf{v}.\hat{\mathbf{r}}(\mathbf{v}.\hat{\mathbf{r}}\cos\theta - \mathbf{v}.\hat{\boldsymbol{\theta}}\sin\theta) - (\sigma_{rr}\cos\theta - \sigma_{r\theta}\sin\theta)]\,d\mu, \quad (22)$$

where

$$\sigma_{rr} = -p + 2\nu\rho\frac{\partial}{\partial r}(\mathbf{v}.\hat{\mathbf{r}}), \quad \sigma_{r\theta} = \nu\rho\left[r\frac{\partial}{\partial r}\left(\frac{\mathbf{v}.\hat{\boldsymbol{\theta}}}{r}\right) + \frac{1}{r}\frac{\partial}{\partial\theta}(\mathbf{v}.\hat{\mathbf{r}})\right]. \quad (23), (24)$$

The expression

$$-2\pi R^2 \int_{-1}^{1} (\sigma_{rr}\cos\theta - \sigma_{r\theta}\sin\theta)\,d\mu$$

occurring in (22) represents the force, in the direction of $\mathbf{F}_0$, exerted on the fluid within the sphere of radius R by the surrounding fluid. Now

$$\int_\tau \frac{\partial}{\partial t}[\rho(\mathbf{v}.\hat{\mathbf{r}}\cos\theta - \mathbf{v}.\hat{\boldsymbol{\theta}}\sin\theta)]\,d\tau = 2\pi\rho\nu\frac{\partial}{\partial t}\int_{-1}^{1}\int_0^R [g - \lambda g_\lambda - \mu g_\mu]\,r\,dr\,d\mu, \quad (25)$$

and after some manipulation involving mainly integration by parts and use of (13) and the fact that, for any non-zero t, $g(\mu,\lambda)\to g_\infty(\mu)$ *as* $r\to 0$, the right-hand side of (25) reduces to

$$2\pi\rho\nu R^2\frac{\partial}{\partial t}\int_{-1}^{1} g[\mu, (\nu t)^{\frac{1}{2}}/R]\,d\mu = \pi\rho\nu^2\int_{-1}^{1}\frac{g_\lambda}{\lambda}d\mu,$$

where $\lambda = (\nu t)^{\frac{1}{2}}/R$, and thus

$$\int_\tau \frac{\partial}{\partial t}[\rho(\mathbf{v}.\hat{\mathbf{r}}\cos\theta - \mathbf{v}.\hat{\boldsymbol{\theta}}\sin\theta)]\,d\tau = \pi\rho\nu^2\int_{-1}^{1}\frac{g_\lambda}{\lambda}d\mu. \quad (26)$$

On substituting the formulae for σ_{rr} and $\sigma_{r\theta}$ and the expression (26) in (22), making use of (2), (4) and (18) and performing some algebra which also involves integration of part of the resulting expression between $\mu = -1$ and $\mu = 1$, we obtain

$$\frac{F_0}{2\pi\rho\nu^2} = \int_{-1}^{1}\left[\frac{1}{2}\left(\frac{g_\lambda}{\lambda} + \frac{g}{\lambda^2}\right) + 2g + \mu(h^* + g_\mu^2) + \lambda g_\lambda g_\mu - \lambda^2 g_{\lambda\lambda}\right]d\mu. \quad (27)$$

For all λ the right-hand side of (27) must be a constant, whose value is given by (10). The expression given by (10) is obtained from (26) from the case $\lambda = \infty$ (steady state) by making use of (7), (9) and (19). If the numerical solution we construct is accurate (10) must be in reasonably good agreement with (27) for all λ.

3. Initial motions

Since the right-hand side of (27) must be a constant, in view of (11), (12) and (19) we must have

$$g \approx \lambda^2 g_0(\mu) \quad \text{for small } \lambda. \quad (28)$$

Also, from (5), (6), the boundary condition (13) and (28) it follows that for small λ

$$g \approx A\lambda^2(1-\mu^2), \quad f \approx 0, \quad (29), (30)$$

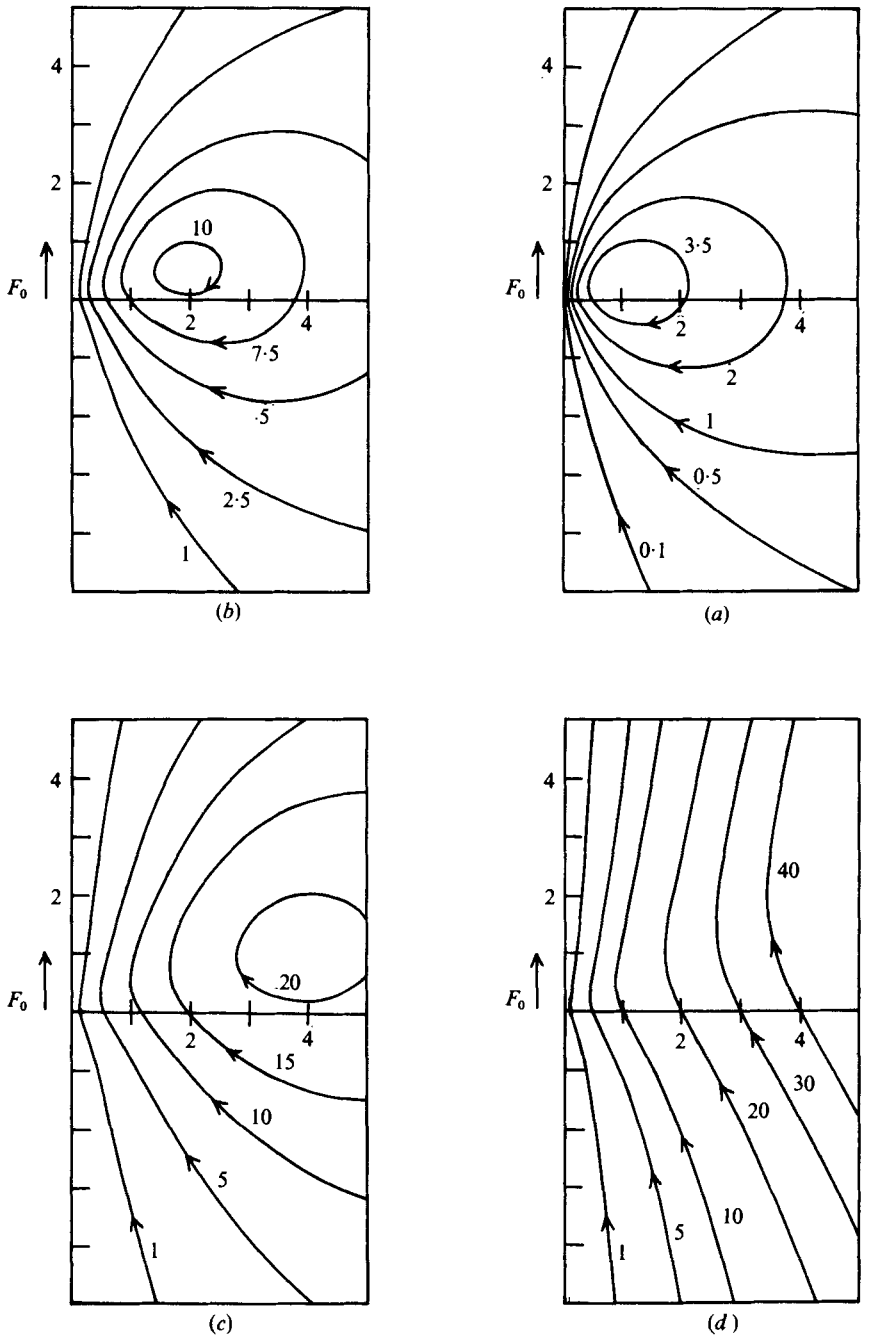

FIGURE 2. Streamlines of the developing flow field for the case $c = 1$ at (*a*) $T = 0{\cdot}5$, (*b*) $T = 1$, (*c*) $T = 2$ and (*d*) $T = \infty$. The numbers on the curves are values of $10\psi/\nu L$. The distances along the axes are in units of L. $F_0 = 11{\cdot}07\pi\rho\nu^2$.

where A is a constant. On substituting (29) and (30) in the expression for h^* and (27), and considering the limit as $\lambda \to 0$, we obtain

$$A = F_0/4\pi\rho\nu^2, \tag{31}$$

$$\psi = \nu r g = \frac{F_0}{4\pi\rho}\frac{t(1-\mu^2)}{r}. \tag{32}$$

Thus the flow field is that of a dipole with axis along the direction of the impressed force; that is, at a given station, initially the fluid viscosity plays no part and the flow field is irrotational, as one might expect.

The expression for A given by (31) is correct provided that $\lambda \ll 1$ and the nonlinear terms of the integrand on the right-hand side of (27) are negligible in comparison with g/λ^2, i.e. (32) is valid when

$$\nu t \ll r^2, \quad F_0 t^2 \ll 4\pi\rho r^4. \tag{33), (34}$$

Also, it follows from (4), (18), (29) and (31) that at $t = 0+$, i.e. as soon as the force F_0 is applied, an impulsive pressure $F_0\mu/4\pi r^2$ is set up in the fluid. The momentum flux $\int p\, d\mathbf{S}$ due to the impulsive pressure through the surface of a sphere of radius R surrounding the origin accounts for one-third of the applied force $\mathbf{F}_0$. Note that, as $t \to 0$, $\mathbf{v} \to 0$ but $\rho\, \partial\mathbf{v}/\partial t = -\nabla p \neq 0$ and the remaining part of $\mathbf{F}_0$ accounts for the sudden increment (from zero at $t = 0-$) in the rate of increase of the linear momentum in the direction of $\mathbf{F}_0$, as can be ascertained from (26). In view of the dipolar nature of the original flow field, for $\nu t \ll R^2$ and $F_0 t^2 \ll 4\pi\rho R^4$, the total linear momentum of the fluid outside the sphere of radius R is zero. For a given non-zero t, $g \sim g_\infty$ as $r \to 0$ [inequalities (33) and (34) are then both reversed]. Thus within the sphere $\mathbf{v}$ is not dipolar everywhere. That is why, at a given time t, the linear momentum and the rate of change of linear momentum of the fluid bounded by the surface of the sphere are not zero.

4. The numerical method

Equations (5) and (6) are the fundamental equations of our problem. These equations are elliptic within the region $-1 < \mu < 1$, $0 < \lambda < \Lambda$, but become parabolic on the boundaries $\mu = \pm 1$ and $\lambda = 0$. Since g is specified on $\lambda = 0$, $\lambda = \Lambda$ and on $\mu = \pm 1$ by (12)–(14), a numerical solution of (6) may, in principle, be obtained relatively easily, once f is specified. The boundary conditions for f are given by (11) and (15)–(17). The solution of (5) is rather complicated, since the form of (16) and (17) requires the solution for f on $\mu = \pm 1$. As described by Sozou & Pickering (1975), it is convenient to transform equations of the form (5) and (6) into equations which are elliptic throughout the region of interest.

For the present problem we employed the transformations

$$\eta = 1-(1-\mu)^{\frac{1}{2}} \quad (0 < \mu \leqslant 1), \tag{35a}$$

$$\eta = (1+\mu)^{\frac{1}{2}}-1 \quad (-1 \leqslant \mu < 0), \tag{35b}$$

$$\xi = \log\lambda. \tag{36}$$

The transformations (35) were used in order to make our equations elliptic on $\mu = \pm 1$.

Relation (36) was primarily employed to provide an increasing (with increasing λ) step length in the λ direction, for a constant step length in the ξ direction. This transformation also eliminates the parabolic nature of our equations on $\lambda = 0$. Thus the equations of our problem become

$$(1+2\eta-\eta^2)F_{\eta\eta}-(2G-2G_\xi+14\eta-7\eta^2-1)F_\eta/(1-\eta)+4F_{\xi\xi} +2[6-e^{-2\xi}-G_\eta/(1-\eta)]F_\xi-6G_\eta F/(1-\eta)=0 \quad (37)$$

and

$$G_{\eta\eta}+G_\eta/(1-\eta)+4(G_{\xi\xi}-G_\xi)/(1+2\eta-\eta^2)=4F(1-\eta)^2 \quad (38)$$

for $0 < \eta \leqslant 1$ and

$$(1-2\eta-\eta^2)F_{\eta\eta}-(2G-2G_\xi+14\eta+7\eta^2+1)F_\eta/(1+\eta)+4F_{\xi\xi} +2[6-e^{-2\xi}-G_\eta/(1+\eta)]F_\xi-6G_\eta F/(1+\eta)=0 \quad (39)$$

and

$$G_{\eta\eta}-G_\eta/(1+\eta)+4(G_{\xi\xi}-G_\xi)/(1-2\eta-\eta^2)=4F(1+\eta)^2 \quad (40)$$

for $-1 \leqslant \eta < 0$, where

$$F(\eta,\xi)=f[\mu(\eta),e^\xi], \quad G(\eta,\xi)=g[\mu(\eta),e^\xi].$$

On $\mu = \eta = 0$, either (37) and (38) or (39) and (40) may be used since both pairs of equations reduce to the corresponding forms of (5) and (6). Alternatively, (5), (6) and (36) (with $\mu = 0$) may be used with $\delta\mu = \delta\eta(2-\delta\eta)$. We adopted the latter approach in our calculations. Since $\lambda = 0$ corresponds to $\xi = -\infty$, the boundary conditions on $\lambda = 0$ were replaced by (29) and (30) on $\xi = \xi_0$, where $\xi_0 = \log\lambda_0$, $\lambda_0 \ll 1$, i.e. we set

$$F(\eta,\xi_0)=0, \quad G(\eta,\xi_0)=(F_0/4\pi\rho\nu^2)\lambda_0^2[1-\mu^2(\eta)]. \quad (41),(42)$$

Equations (13)–(15) were transformed to

$$G(1,\xi)=G(-1,\xi)=0, \quad (43)$$

$$G(\eta,\Xi)=g_\infty(\mu), \quad F(\eta,\Xi)=g''_\infty(\mu), \quad (44),(45)$$

where $\Xi = \log\Lambda$. Conditions (16) and (17) were replaced by

$$F_\eta(1,\xi)=0=F_\eta(-1,\xi) \quad (46)$$

together with the requirements that

$$F_\eta/(1-\eta)=-F_{\eta\eta}, \quad G_\eta/(1-\eta)=-G_{\eta\eta} \quad \text{as} \quad \eta\to 1 \quad (47)$$

and

$$F_\eta/(1+\eta)=F_{\eta\eta}, \quad G_\eta(1+\eta)=G_{\eta\eta} \quad \text{as} \quad \eta\to -1. \quad (48)$$

The numerical techniques used to express (37)–(40) in finite-difference form were very similar to those employed previously (Sozou & Pickering 1975) and our equations were solved iteratively, by successive over-relaxation, as follows. We specified an initial approximation to G and solved (37) and (39) for F. This solution was then used to solve (38) and (40) for a better approximation to G and so on until convergence. Convergence was assumed when two successive iterations produced changes of less than 10^{-3} in F and less than 0·1 % in G. We set $\lambda_0 = 10^{-2}$ ($\xi_0 \simeq -4{\cdot}6$) and $\Xi = 2$ ($\Lambda \simeq 7{\cdot}4$). The step lengths in the ξ and η directions were $\frac{1}{64}(\Xi-\xi_0) \approx 0{\cdot}103$ and $\frac{1}{11}$, respectively.

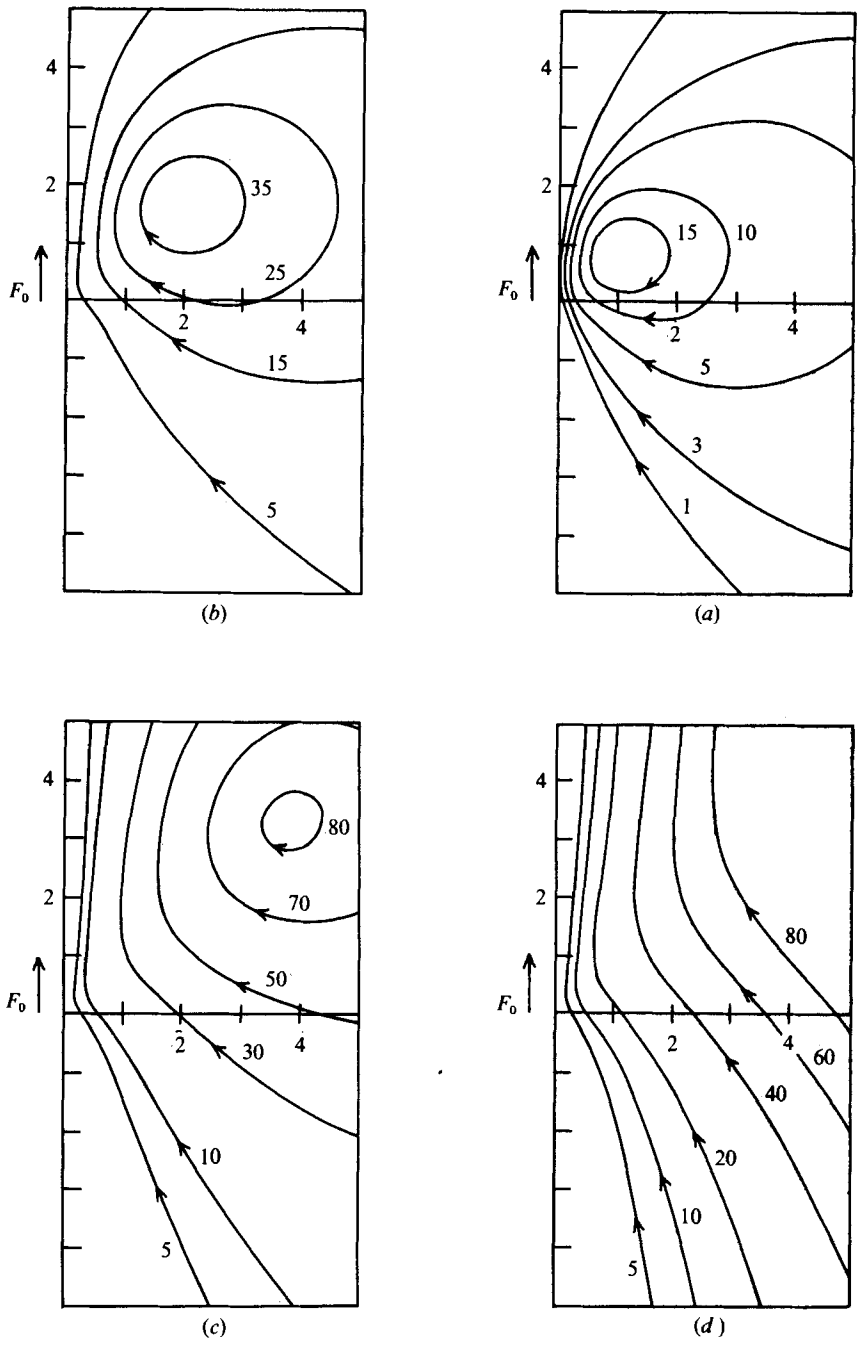

FIGURE 3. Streamlines of the developing flow field for the case $c = 0{\cdot}2$ at (*a*) $T = 0{\cdot}5$, (*b*) $T = 1$, (*c*) $T = 2$ and (*d*) $T = \infty$. The numbers on the curves are values of $10\psi/\nu L$. The distances along the axes are in units of L. $F_0 = 49{\cdot}76\pi\rho\nu^2$.

5. Results and discussion

We performed computations for various c's in the range 0·2–10. When $c = O(10)$, $|f| \ll 1$, $0 \leqslant g \ll 1$ and the flow field is essentially linear. For that case the numerical solution we constructed converges rapidly. As c decreases the convergence of the solution becomes slower, especially for $c < 0{\cdot}5$, where we had to under-relax in order to obtain a convergent solution. We believe that our computations bring out all the essential features of the development of the flow of the round laminar jet, and we need not proceed to values of $c \ll 0{\cdot}2$, where the convergence of the solution is very slow.

As already suggested in § 2, an indication of the accuracy of our numerical solution can be obtained by checking for the satisfaction of (21) and, for all λ, of (27). Our computations, using second-order finite-difference formulae for the derivatives and Simpson's rule for the integration, have shown that these equations are approximately satisfied. For $c = 10$ and $c = 1$ our $h(\mu, \Lambda)$ in general differs by less than 3 % from $h(\mu, \infty)$. For $c = 0{\cdot}2$ this is the case only for $\mu < \frac{1}{3}$. For $\mu > \frac{1}{3}$ the percentage difference between $h(\mu, \Lambda)$ and $h(\mu, \infty)$ increases with μ to a maximum of about 18 % and then decreases as μ increases further. This is probably due to the fact that, for the case $c = 0{\cdot}2$, for a specified λ, say λ_1, where $\lambda_1 \geqslant O(1)$, the rate of change of $f(\mu, \lambda_1)$ with respect to μ is large for $\mu > \frac{1}{3}$, and increases as μ increases. Thus, with the finite-difference scheme used, as μ increases beyond $\frac{1}{3}$, the accuracy of the expression $(1-\mu^2) f_\mu$ occurring in (19) is reduced, except near $\mu = 1$. For the complete range of λ, and all values of c used, the right-hand side of (27) differed by less than 10 % from its expected constant value corresponding to the right-hand side of (10). Indeed, for most of the range of λ the right-hand side of (27) differed by not more than 3–4 % from the expected constant.

For all values of c used, we found that at $\lambda = 3{\cdot}5$ the values of $g(\mu, \lambda)$ and $f(\mu, \lambda)$ differed by less than 10 % from their respective steady-state values. Indeed, for many values of μ, $g(\mu, 3{\cdot}5)$ and $f(\mu, 3{\cdot}5)$ differed by only 2–3 % from $g_\infty(\mu)$ and $f_\infty(\mu)$ respectively. This justifies our setting the steady state at $\lambda = \Lambda = e^2 \approx 7{\cdot}4$.

Streamlines of the flow fields which we computed are shown in figures 1–3, for various times, for the cases $c = 10$, 1 and 0·2. When $c = O(10)$, the flow field is very nearly symmetrical about the equatorial plane $\mu = 0$ as is clearly seen by inspection of figure 1. When $c \ll 10$ the flow field is not symmetric about the plane $\mu = 0$ and as c decreases the asymmetry increases, except at times such that (33) and (34) are satisfied, when the field is, in effect, that of a dipole as described in § 3.

In the early stages of development the streamlines are closed loops, as is seen from figures 1–3. This closed-loop structure of the flow field can also be deduced from the fact that, at a given time t, λ is large near the origin and there $g \sim g_\infty$ and the flow field has a structure similar to the steady state. The streamlines (except the axial one) intersect the plane $\mu = 0$ at $r \neq 0$. For r sufficiently large that (33) and (34) are satisfied, the flow field has a dipole-like structure whose streamlines must join up with those which intersect the plane $\mu = 0$ nearer the origin, i.e. the streamlines form closed loops. The limiting loop (of zero length) represents a point at which ψ has a maximum, i.e. a stagnation point (in effect a stagnation ring about the axis of symmetry of the problem). Since we can write $\psi = \nu(\nu t)^{\frac{1}{2}} g(\mu, \lambda)/\lambda$ the maximum value of ψ must correspond to a particular λ, say λ_m, and a particular μ, say, μ_m. As t increases the velocity field develops and the stagnation point moves to infinity along the line $\mu = \mu_m$ with speed

$\nu^{\frac{1}{2}}/2\lambda_m t^{\frac{1}{2}}$. Our computations have shown that the smaller the value of c, i.e. the larger the applied force, the smaller is the value of λ_m. Indeed, for the cases $c = 10$, 1 and 0·2 the corresponding values of λ_m are 0·56, 0·53 and 0·39. This is also evident from figures 1–3. Inspection of these figures shows that for a particular dimensionless time $T = (\nu t)^{\frac{1}{2}}/L$, where L is a characteristic length, say $T = 1$, the distance from the origin of the limiting streamline (maximum value of ψ) increases as c decreases. This implies that the larger the applied force the faster the stagnation point moves to infinity and the faster the steady state is established.

The development of the flow field discussed above is similar to that of the magneto-hydrodynamic flow due to the discharge of an electric current in a semi-infinite fluid (Sozou & Pickering 1975). In that case, however, the corresponding value of λ_m increases as the discharged current increases, i.e. as the applied force increases. This behaviour of λ_m is at variance with what happens in the present investigation but in the earlier problem the driving force is distributed throughout the fluid and is not concentrated at one point, as is the case here.

We are indebted to Mr D. J. Mullings for programming assistance.

REFERENCES

BATCHELOR, G. K. 1967 *Introduction to Fluid Dynamics*. Cambridge University Press.

LANDAU, L. D. & LIFSHITZ, E. M. 1959 *Fluid Mechanics*. Pergamon.

LIGHTHILL, M. J. 1973 *J. Fluid Mech.* **60**, 1.

SOZOU, C. & PICKERING, W. M. 1975 *J. Fluid Mech.* **70**, 509.

SQUIRE, H. B. 1951 *Quart. J. Mech. Appl. Math.* **4**, 321.

WHITHAM, G. B. 1963 In *Laminar Boundary Layers* (ed. L. Rosenhead), pp. 114–162. Oxford: Clarendon Press.